Electronic Supporting Information

An organic chromophore modified samarium-containing polyoxometalates: excitation-dependent color tunable behavior from organics to lanthanide ion

Hechen Wu[1,2], Bing Yan[1], Rongchang Liang[1], Vikram Singh[1], Pengtao Ma*[1] Jingping Wang[1] and Jingyang Niu*[1]

[1]*Henan Key Laboratory of Polyoxometalate Chemistry, Institute of Molecular and Crystal Engineering, College of Chemistry and Chemical Engineering, Henan University, Kaifeng, Henan 475004, P. R. China*
[2]*Department of Chemistry, Fudan University, Shanghai 200433, China*

Photoluminescence section

Tables

Figures

Photoluminescence section

The CIE 1931 chromaticity coordinates and CCT are important optical parameters in research of PL properties of luminescent complexes. The CCT can be calculated by the following equations (1):

$n = (x - x_e)/(y_e - y)$

$CCT = 499.0n^3 + 3525.0n^2 + 6823.3n + 5520.22$ (1)

Where $x_e = 0.3320$; $y_e = 0.1858$; x, y are the CIE 1931 chromaticity coordinates.

Table S1. Selected bond lengths (Å) of **1**.

Bond	Length	Bond	Length
Sm(1)-O(13)	2.383(9)	K(1)-O(6)	2.735(10)
Sm(1)-O(16)	2.326(9)	K(1)-O(30)[a]	2.797(9)
Sm(1)-O(19)	2.343(9)	K(1)-O(41)[a]	2.709(11)
Sm(1)-O(30)	2.393(9)	K(1)-O(4W)	2.686(14)
Sm(1)-O(40)	2.502(10)	K(2)-O(3)[b]	2.717(11)
Sm(1)-O(41)	2.526(10)	K(2)-O(7)	2.847(11)
Sm(1)-O(1W)	2.383(9)	K(2)-O(8)[c]	2.793(11)
Sm(1)-O(2W)	2.326(9)	K(2)-O(8W)	2.78(2)
		K(2)-O(9W)	2.72(2)
W(1)-O(1)	1.697(11)	W(6)-O(34)	1.894(9)
W(1)-O(20)	1.937(10)	W(6)-O(35)	1.900(9)
W(1)-O(24)	1.911(10)	W(6)-O(37)	2.422(9)
W(1)-O(27)	1.901(9)	W(7)-O(7)	1.708(11)
W(1)-O(32)	1.889(9)	W(7)-O(21)	1.896(10)
W(1)-O(36)	2.399(9)	W(7)-O(23)	1.911(9)
W(2)-O(2)	1.726(10)	W(7)-O(28)	1.939(10)
W(2)-O(19)	1.768(9)	W(7)-O(33)	1.895(9)
W(2)-O(22)	2.047(9)	W(7)-O(38)	2.420(9)
W(2)-O(26)	1.902(9)	W(8)-O(8)	1.711(10)
W(2)-O(27)	1.952(9)	W(8)-O(14)	1.898(9)
W(2)-O(36)	2.470(9)	W(8)-O(18)	1.931(9)
W(3)-O(3)	1.699(11)	W(8)-O(28)	1.947(10)
W(3)-O(17)	1.901(10)	W(8)-O(29)	1.826(9)
W(3)-O(20)	1.892(9)	W(8)-O(38)	2.473(9)
W(3)-O(21)	1.936(10)	W(9)-O(9)	1.702(11)
W(3)-O(22)	1.842(9)	W(9)-O(18)	1.923(10)
W(3)-O(36)	2.524(9)	W(9)-O(23)	1.952(10)
W(4)-O(4)	1.704(11)	W(9)-O(24)	1.905(9)
W(4)-O(12)	1.927(10)	W(9)-O(25)	1.801(9)
W(4)-O(15)	1.838(9)	W(9)-O(38)	2.400(8)
W(4)-O(17)	1.901(10)	W(10)-O(10)	1.710(10)
W(4)-O(33)	1.949(10)	W(10)-O(29)	2.042(9)
W(4)-O(37)	2.502(9)	W(10)-O(30)	1.773(9)
W(5)-O(5)	1.716(10)	W(10)-O(31)	1.900(9)
W(5)-O(15)	2.042(9)	W(10)-O(34)	1.941(8)
W(5)-O(16)	1.772(9)	W(10)-O(39)	2.385(9)
W(5)-O(26)	1.912(9)	W(11)-O(11)	1.719(10)
W(5)-O(35)	1.969(9)	W(11)-O(13)	1.766(9)
W(5)-O(37)	2.439(8)	W(11)-O(25)	2.064(9)
W(6)-O(6)	1.734(10)	W(11)-O(31)	1.933(10)
W(6)-O(12)	1.922(10)	W(11)-O(32)	1.918(9)

W(6)-O(14)	1.929(9)	W(11)-O(39)	2.354(8)

symmetry code a = 2-X,1-Y,1-Z; b = 1-X,1-Y,2-Z; c = 2-X,1-Y,2-Z.

Table S2. Selected bond angels (°) of **1**.

Bond	Angel	Bond	Angel	Bond	Angel
O(1)-W(1)-O(20)	101.0(5)	O(17)-W(4)-O(12)	155.0(4)	O(14)-W(8)-O(38)	84.9(3)
O(1)-W(1)-O(24)	101.7(5)	O(17)-W(4)-O(33)	84.3(4)	O(18)-W(8)-O(28)	85.7(4)
O(1)-W(1)-O(27)	101.3(5)	O(17)-W(4)-O(37)	84.6(4)	O(18)-W(8)-O(38)	72.0(3)
O(1)-W(1)-O(32)	102.7(5)	O(33)-W(4)-O(37)	82.5(4)	O(28)-W(8)-O(38)	72.1(4)
O(1)-W(1)-O(36)	172.8(4)	O(5)-W(5)-O(15)	97.7(4)	O(29)-W(8)-O(14)	88.4(4)
O(20)-W(1)-O(36)	74.3(3)	O(5)-W(5)-O(16)	104.0(5)	O(29)-W(8)-O(18)	90.1(4)
O(24)-W(1)-O(20)	85.7(4)	O(5)-W(5)-O(26)	102.7(4)	O(29)-W(8)-O(28)	155.5(4)
O(24)-W(1)-O(36)	83.7(4)	O(5)-W(5)-O(35)	101.9(4)	O(29)-W(8)-O(38)	83.7(4)
O(27)-W(1)-O(20)	87.9(4)	O(5)-W(5)-O(37)	167.2(4)	O(9)-W(9)-O(18)	100.2(5)
O(27)-W(1)-O(24)	156.9(4)	O(15)-W(5)-O(37)	70.8(3)	O(9)-W(9)-O(23)	101.4(5)
O(27)-W(1)-O(36)	73.3(4)	O(16)-W(5)-O(15)	158.2(4)	O(9)-W(9)-O(24)	102.9(5)
O(32)-W(1)-O(20)	156.0(4)	O(16)-W(5)-O(26)	93.1(4)	O(9)-W(9)-O(25)	103.5(5)
O(32)-W(1)-O(24)	86.1(4)	O(16)-W(5)-O(35)	91.7(4)	O(9)-W(9)-O(38)	171.0(4)
O(32)-W(1)-O(27)	90.8(4)	O(16)-W(5)-O(37)	87.4(4)	O(18)-W(9)-O(23)	84.7(4)
O(32)-W(1)-O(36)	82.3(3)	O(26)-W(5)-O(15)	84.4(4)	O(18)-W(9)-O(38)	73.9(3)
O(2)-W(2)-O(19)	103.0(5)	O(26)-W(5)-O(35)	153.0(4)	O(23)-W(9)-O(38)	71.5(3)
O(2)-W(2)-O(22)	96.5(4)	O(26)-W(5)-O(37)	82.3(3)	O(24)-W(9)-O(18)	156.5(4)
O(2)-W(2)-O(26)	102.6(4)	O(35)-W(5)-O(15)	81.3(4)	O(24)-W(9)-O(23)	86.4(4)
O(2)-W(2)-O(27)	102.9(4)	O(35)-W(5)-O(37)	71.4(3)	O(24)-W(9)-O(38)	82.7(3)
O(2)-W(2)-O(36)	165.8(4)	O(6)-W(6)-O(12)	100.5(4)	O(25)-W(9)-O(18)	91.1(4)
O(19)-W(2)-O(22)	160.5(4)	O(6)-W(6)-O(14)	103.2(4)	O(25)-W(9)-O(23)	155.1(4)
O(19)-W(2)-O(26)	93.0(4)	O(6)-W(6)-O(34)	103.5(4)	O(25)-W(9)-O(24)	88.0(4)
O(19)-W(2)-O(27)	93.1(4)	O(6)-W(6)-O(35)	98.4(4)	O(25)-W(9)-O(38)	83.7(4)
O(19)-W(2)-O(36)	90.2(4)	O(6)-W(6)-O(37)	169.6(4)	O(10)-W(10)-O(29)	94.5(4)
O(22)-W(2)-O(36)	70.3(3)	O(12)-W(6)-O(14)	86.7(4)	O(10)-W(10)-O(30)	103.2(4)
O(26)-W(2)-O(22)	83.2(4)	O(12)-W(6)-O(37)	73.6(4)	O(10)-W(10)-O(31)	100.6(4)
O(26)-W(2)-O(27)	151.6(4)	O(14)-W(6)-O(37)	85.3(3)	O(10)-W(10)-O(34)	102.3(4)
O(26)-W(2)-O(36)	81.5(3)	O(34)-W(6)-O(12)	156.0(4)	O(10)-W(10)-O(39)	171.0(4)
O(27)-W(2)-O(22)	81.9(4)	O(34)-W(6)-O(14)	87.0(4)	O(29)-W(10)-O(39)	80.5(3)
O(27)-W(2)-O(36)	70.8(3)	O(34)-W(6)-O(35)	90.7(4)	O(30)-W(10)-O(29)	161.8(4)
O(3)-W(3)-O(17)	103.0(5)	O(34)-W(6)-O(37)	82.8(3)	O(30)-W(10)-O(31)	94.7(4)
O(3)-W(3)-O(20)	101.0(5)	O(35)-W(6)-O(12)	86.6(4)	O(30)-W(10)-O(34)	91.3(4)
O(3)-W(3)-O(21)	102.8(5)	O(35)-W(6)-O(14)	158.2(4)	O(30)-W(10)-O(39)	82.4(4)
O(3)-W(3)-O(22)	103.1(5)	O(35)-W(6)-O(37)	72.9(3)	O(31)-W(10)-O(29)	85.7(4)
O(3)-W(3)-O(36)	171.2(4)	O(7)-W(7)-O(21)	103.5(5)	O(31)-W(10)-O(34)	154.3(4)
O(17)-W(3)-O(21)	84.2(4)	O(7)-W(7)-O(23)	100.5(4)	O(31)-W(10)-O(39)	71.6(3)
O(17)-W(3)-O(36)	84.6(4)	O(7)-W(7)-O(28)	100.0(5)	O(34)-W(10)-O(29)	81.1(4)

O(20)-W(3)-O(17)	155.3(4)	O(7)-W(7)-O(33)	103.2(5)	O(34)-W(10)-O(39)	84.4(3)
O(20)-W(3)-O(21)	85.1(4)	O(7)-W(7)-O(38)	169.9(4)	O(11)-W(11)-O(13)	102.0(5)
O(20)-W(3)-O(36)	72.0(3)	O(21)-W(7)-O(23)	88.6(4)	O(11)-W(11)-O(25)	95.8(4)
O(21)-W(3)-O(36)	82.3(4)	O(21)-W(7)-O(28)	156.5(4)	O(11)-W(11)-O(31)	100.1(4)
O(22)-W(3)-O(17)	90.5(4)	O(21)-W(7)-O(38)	83.2(4)	O(11)-W(11)-O(32)	102.3(4)
O(22)-W(3)-O(20)	89.4(4)	O(23)-W(7)-O(28)	86.6(4)	O(11)-W(11)-O(39)	170.7(4)
O(22)-W(3)-O(21)	154.1(4)	O(23)-W(7)-O(38)	71.7(4)	O(13)-W(11)-O(25)	162.2(4)
O(22)-W(3)-O(36)	72.0(3)	O(28)-W(7)-O(38)	73.5(4)	O(13)-W(11)-O(31)	94.3(4)
O(4)-W(4)-O(12)	101.2(5)	O(33)-W(7)-O(21)	87.1(4)	O(13)-W(11)-O(32)	94.3(4)
O(4)-W(4)-O(15)	102.0(4)	O(33)-W(7)-O(23)	156.3(4)	O(13)-W(11)-O(39)	83.7(4)
O(4)-W(4)-O(17)	103.2(5)	O(33)-W(7)-O(28)	88.0(4)	O(25)-W(11)-O(39)	78.9(3)
O(4)-W(4)-O(33)	103.1(5)	O(33)-W(7)-O(38)	84.6(4)	O(31)-W(11)-O(25)	83.9(4)
O(4)-W(4)-O(37)	170.8(4)	O(8)-W(8)-O(14)	102.4(4)	O(31)-W(11)-O(39)	71.8(3)
O(12)-W(4)-O(33)	85.2(4)	O(8)-W(8)-O(18)	100.4(4)	O(32)-W(11)-O(25)	80.3(4)
O(12)-W(4)-O(37)	71.6(4)	O(8)-W(8)-O(28)	100.7(5)	O(32)-W(11)-O(31)	153.7(4)
O(15)-W(4)-O(12)	88.2(4)	O(8)-W(8)-O(29)	103.7(4)	O(32)-W(11)-O(39)	84.5(3)
O(15)-W(4)-O(17)	91.8(4)	O(8)-W(8)-O(38)	169.6(4)	O(15)-W(4)-O(37)	72.3(3)
O(15)-W(4)-O(33)	154.8(4)	O(14)-W(8)-O(18)	156.8(4)	O(14)-W(8)-O(28)	86.1(4)

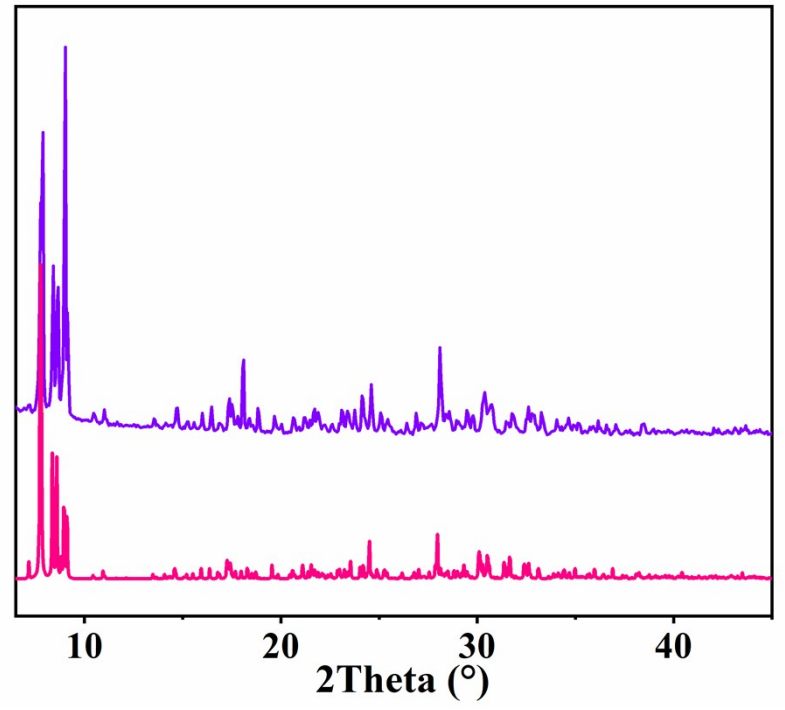

Fig. S1. Simulated single-crystal PXRD of **1** (pink) and experimental PXRD patterns of **1** (violet).

As shown in Fig. S1, the experimental PXRD patterns of **1** is well consistent with the simulated PXRD patterns of **1** that originated from the single-crystal X-ray diffraction structural analyses, evidencing that the experimental samples are in good phase purity.

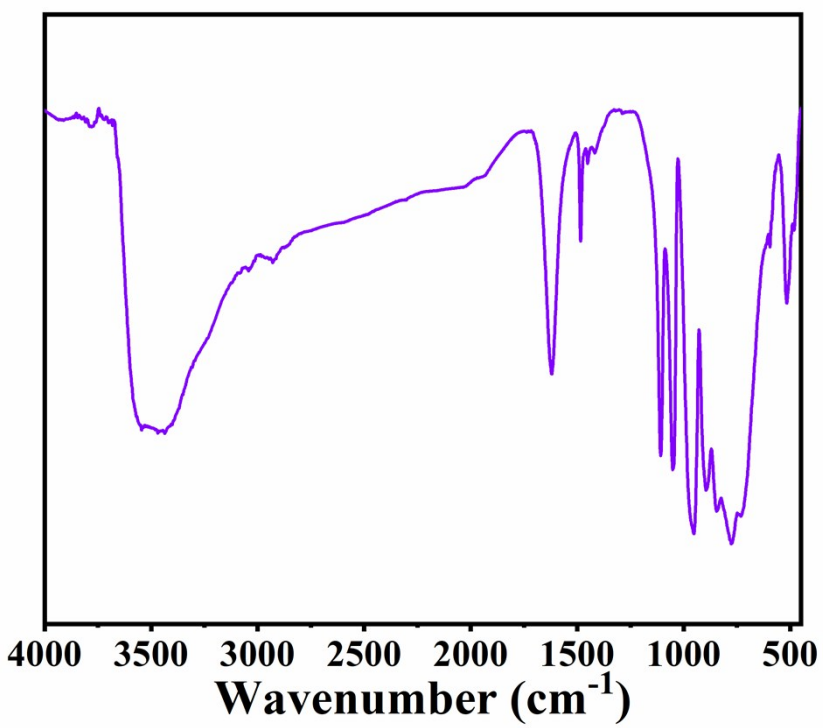

Fig. S2. FTIR spectroscopy of **1**.

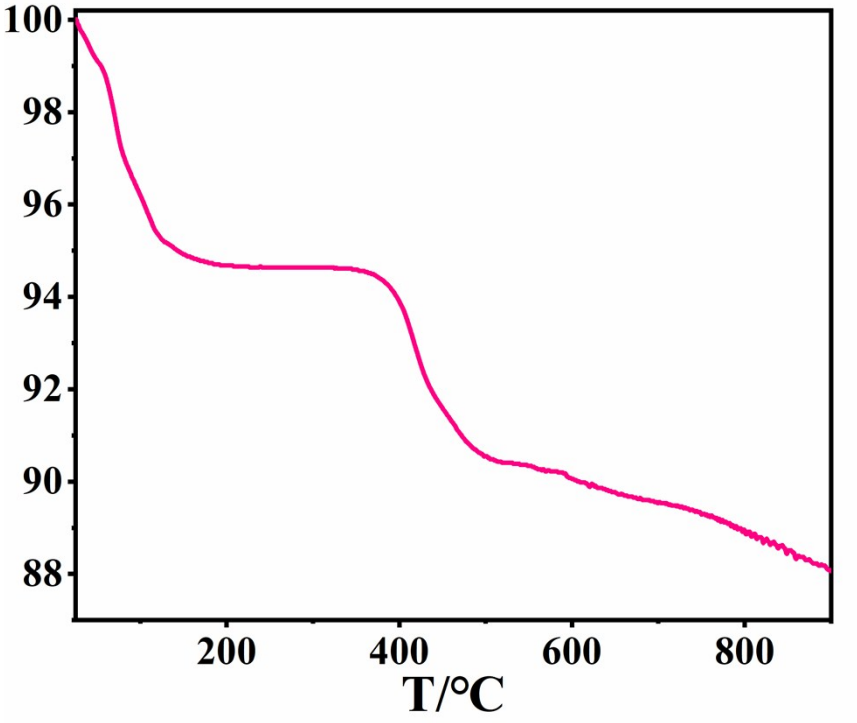

Fig. S3. TGA curve of **1**.

The TGA curve of **1** displays a weight loss from 25 to 140 °C, corresponding to the removal of eleven lattice water (calcd 6.05%). The other weight loss from 140 to 900 °C can be attributed to the loss of coordinated water and $[N(CH_3)_4]^+$ countercations, and the oxidation of organic benzoic acid and partial decomposition of POM skeleton.

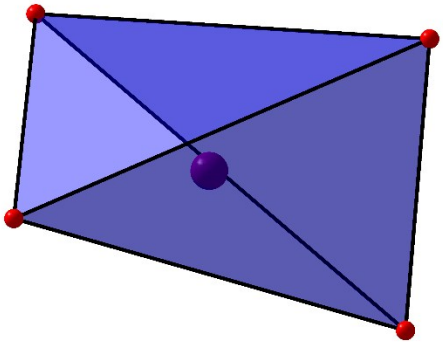

Fig. S4. The coordination environment of K1 ion. (color codes: K1, violet; O, red).

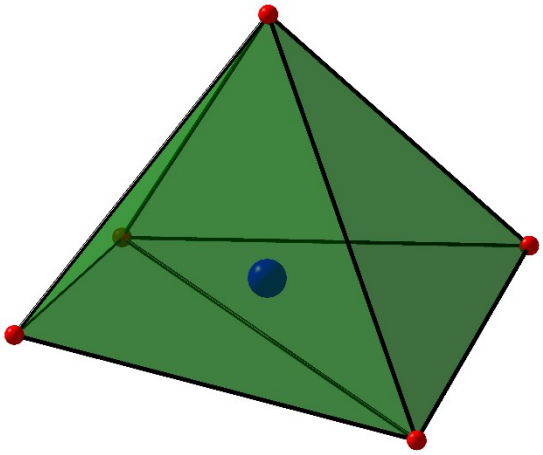

Fig. S5. The coordination environment of K2 ion. (color codes: K2, blue; O, red).

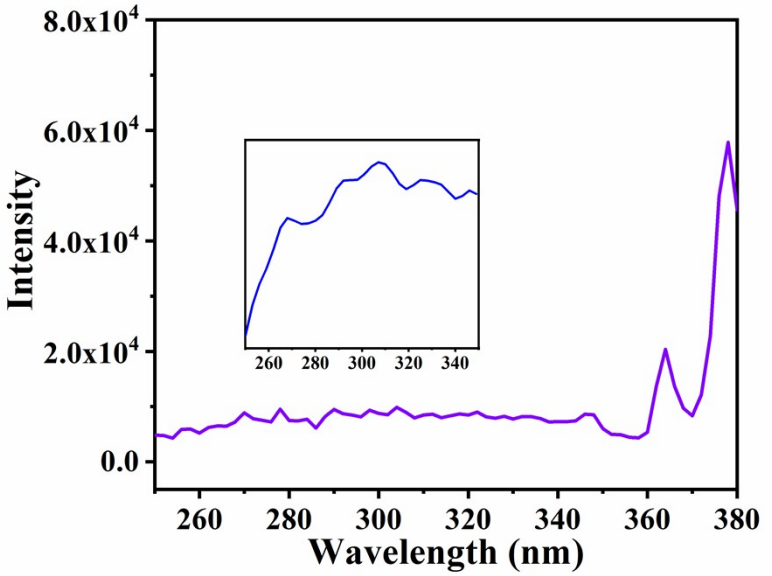

Fig. S6. The excitation spectrum of **1** recorded under emission at 599 nm.

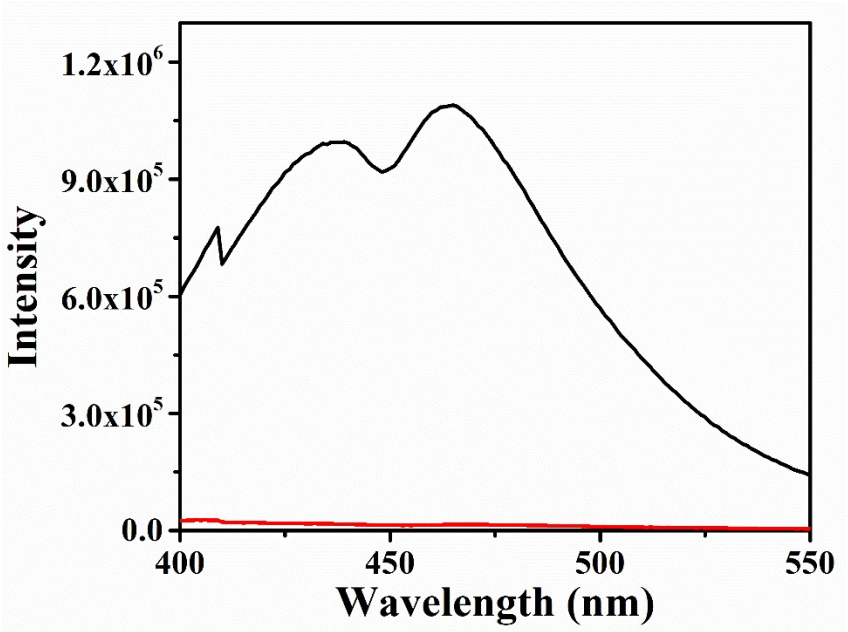

Fig. S7. The photoluminescence emission spectra of benzoic acid ligand and $K_{14}[P_2W_{19}O_{69}(H_2O)]\cdot 24H_2O$ precursor under excitation at 310 nm.

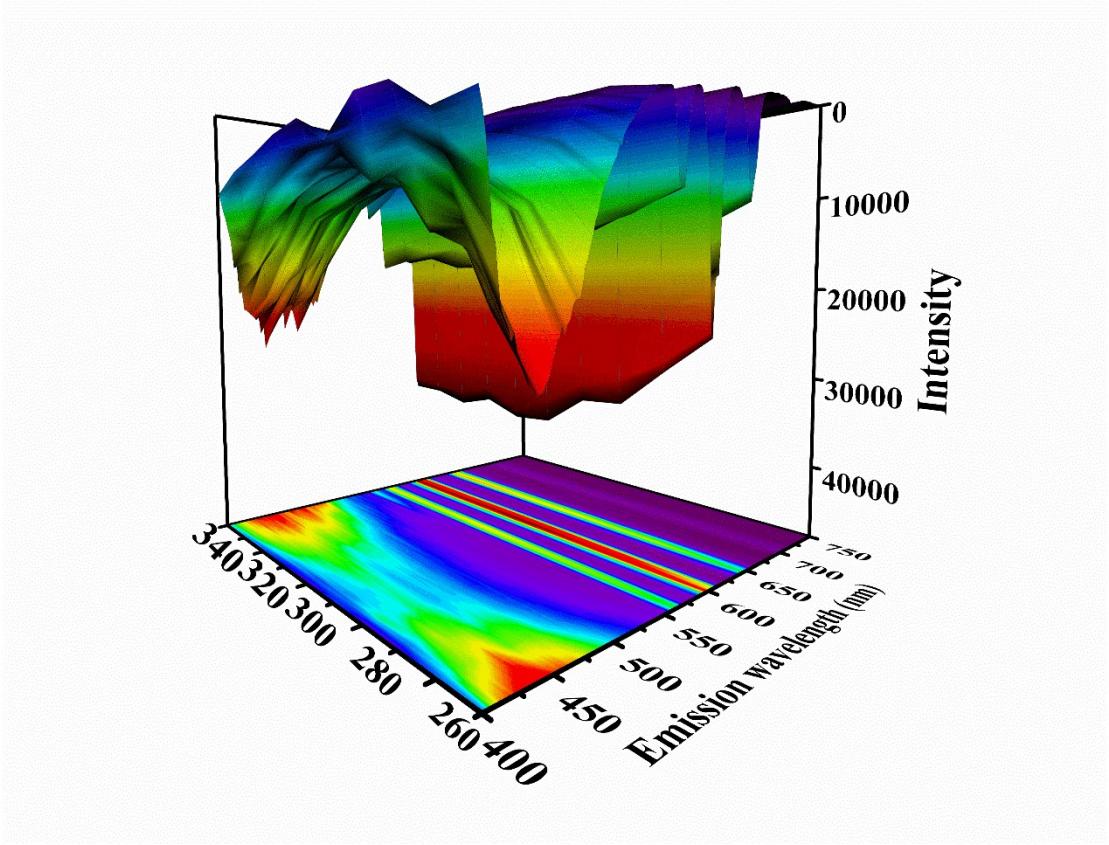

Fig. S8. A view of 3D color surface plots and corresponding 2D diagrams of photoluminescence excitation and emission map (EEM) of **1**.

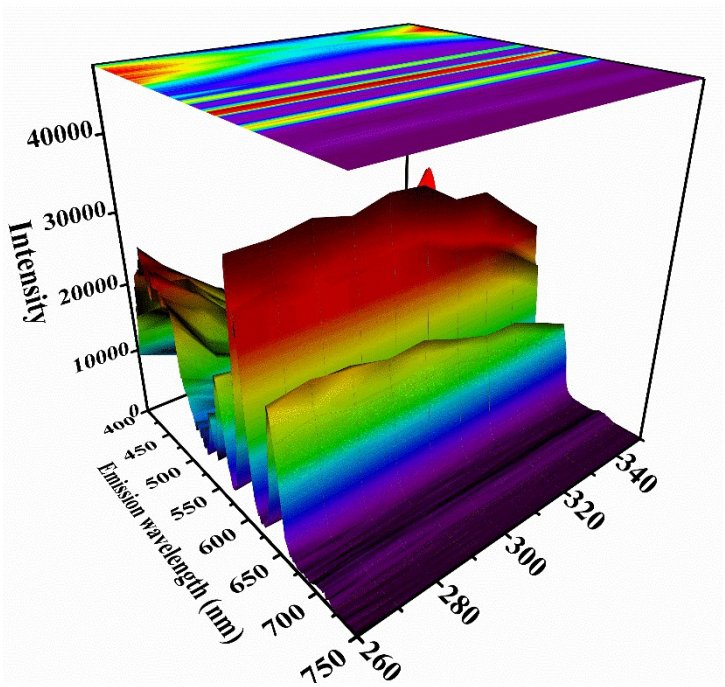

Fig. S9. A view of 3D color surface plots and corresponding 2D diagrams of photoluminescence excitation and emission map (EEM) of **1**.

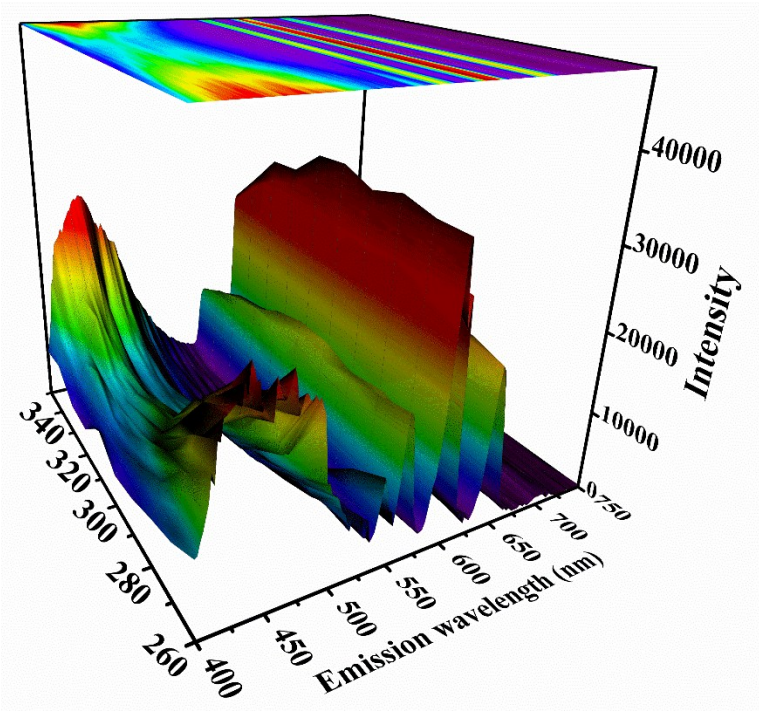

Fig. S10. A view of 3D color surface plots and corresponding 2D diagrams of photoluminescence excitation and emission map (EEM) of **1**.